ELECTRONIC SUPPLEMENTARY INFORMATION (ESI)

Indium(III)/2-benzoylpyridine chemistry: interesting indium(III) bromide-assisted transformations of the ligand

Christina Stamou[a], Zoi G. Lada[b], Christos T. Chasapis[c], Dionissios Papaioannou, Pierre Dechambenoit[d] and Spyros P. Perlepes*[a, b]*

[a.] *Department of Chemistry, University of Patras, 26504 Patras, Greece. E-mail: perlepes@upatras.gr*
[b.] *Institute of Chemical Engineering Sciences (ICE-HT), Foundation for Research and Technology-Hellas (FORTH), P.O. Box 1414, Platani, 26504 Patras, Greece.*
[c.] *NMR Facility, Instrumental Analysis Laboratory, School of Natural Sciences, University of Patras, 26504 Patras, Greece.*
[d.] *Centre de Recherche Paul Pascal, UMR 5031, CNRS, University of Bordeaux, 33600 Pessac, France.*

Contents

Contents

Table S1 Crystallographic data for compounds 1, 3, 4

Parameter	Complex **1**	Complex **3**	Complex **4**
Formula	$C_{26}H_{24}Cl_3InN_2O_3$	$C_{24}H_{17}Br_4InN_2O_2$	$C_{28}H_{32}Br_4In_2N_2O_4$
F_w	633.64	799.85	1009.83
Crystal colour	Colourless	Yellow	Colourless
Crystal size (mm)	0.46x0.15x0.05	0.15x0.02x0.01	0.32x0.08x0.03
Crystal system	Monoclinic	Monoclinic	Monoclinic
Space group	$P2_1/c$	$C2/c$	$P2_1/c$
Temperature/K	120	120	120
a/Å	17.5180(9)	34.562(4)	12.421(9)
b/Å	7.7740(4)	7.6912(10)	10.4041(7)
c/Å	19.4933(9)	19.859(3)	25.5262(19)
β/°	100.390(2)	108.002(14)	90.439(4)
V/Å^3	2611.2(2)	5020.5(12)	3298.8(4)
Z	4	8	4
I_{calcd}	1.612	2.116	2.033
Radiation/μ (mm^{-1})	Mo Ka/1.243	Mo Ka/7.333	Mo Ka/6.278
ϑ_{min}-ϑ_{max}/°	2.124-28.906	2.479-19.933	1.596-27.556
Reflns collected/unique	86266/6788	36527/2247	153532/7611
Completeness to 2ϑ	0.985	0.966	0.988
R_{int}	0.0725	0.1802	0.0456
Refined parameters/ restraints	320/1	298/108	369/2
R_1[a] (I>2σ(I))	0.0250	0.0602	0.0393
wR_2[b] (all data)	0.0554	0.1175	0.0916
GOF (F^2)	1.028	1.129	1.127

[a] $R_1 = \Sigma||F_O|-|F_C||/\Sigma|F_O|$. [b] $wR_2 = \{\Sigma w(F_O^2-F_c^2)^2/\Sigma w(F_O^2)^2\}^{1/2}$.

Table S2 Selected bond distances, bond angles and intermolecular interactions in complex **1**

Distances in Å		*Selected angles in °*	
In1 O2	2.2051(13)	O2 In1 N1	78.79(5)
In1 N1	2.2991(15)	O2 In1 O1	85.98(4)
In1 O1	2.3623(12)	N1 In1 O1	68.96(5)
In1 Cl3	2.3926(5)	O2 In1 Cl3	91.74(4)
In1 Cl2	2.4053(4)	N1 In1 Cl3	157.99(4)
In1 Cl1	2.4419(5)	O1 In1 Cl3	90.77(3)
O1 C6	1.234(2)	O2 In1 Cl2	90.09(4)
O3 C18	1.217(2)	N1 In1 Cl2	93.81(4
		O1 In1 Cl2	162.75(3)
O1 N2 (H-bond)	2.675(1)	Cl3 In1 Cl2	106.143(17)
C2 Cl1	3.364(1)	O2 In1 Cl1	166.01(3)
O3 C20	3.502(1)	N1 In1 Cl1	88.48(4)
O3 C13	3.312(1)	O1 In1 Cl1	84.03(3)
		Cl3 In1 Cl1	98.153(18)
		Cl2 In1 Cl1	96.588(17)

Table S3 Selected bond distances, bond angles and intermolecular interactions in complex **3**

Distances in Å		*Selected angles in °*	
In1 N1	2.313(13)	N1 In1 O1	69.2(5)
In1 O1	2.344(11)	N1 In1 Br4	158.2(4)
In1 Br4	2.563(2)	O1 In1 Br4	89.1(3)
In1 Br3	2.592(2)	N1 In1 Br3	95.4(4)
In1 Br2	2.623(3)	O1 In1 Br3	164.6(3)
In1 Br1	2.647(2)	Br4 In1 Br3	106.30(8)
O1 C6	1.251(19)	N1 In1 Br2	87.2(3)
O2 C13	1.18(2)	O1 In1 Br2	86.5(3)
N2 C19	1.41(2)	Br4 In1 Br2	93.56(7)
		Br3 In1 Br2	93.91(8)
C15 C22	3.382(1)	N1 In1 Br1	84.9(3)
C16 C21	3.284(1)	O1 In1 Br1	84.6(3)
C10 O2	3.201(1)	Br4 In1 Br1	91.33(7)
C20 Br4	3.648(1)	Br3 In1 Br1	93.33(8)
C18 Br3	3.627(1)	Br2 In1 Br1	169.77(9)
C18 Br2	3.533(1)		

Table S4 Selected bond distances, bond angles and intermolecular interactions in complex **4**

Distances in Å		*Selected angles in °*	
In2 O1	2.135(3)	O1 In2 O2	73.33(12)
In2 O2	2.161(3)	O1 In2 N2	145.22(14)
In2 N2	2.235(4)	O2 In2 N2	73.86(13)
In2 O4	2.291(4)	O1 In2 O4	81.90(13)
In2 Br3	2.5319(6)	O2 In2 O4	82.05(13)
In2 Br4	2.6220(6)	N2 In2 O4	82.49(14)
In1 O2	2.134(3)	O1 In2 Br3	110.78(9)
In1 O1	2.184(3)	O2 In2 Br3	171.99(9)
In1 N1	2.248(4)	N2 In2 Br3	100.53(11)
In1 O3	2.281(4)	O4 In2 Br3	91.63(9)
In1 Br1	2.5372(6)	O1 In2 Br4	94.54(9)
In1 Br2	2.6138(6)	O2 In2 Br4	91.89(9)
O2 C18	1.406(5)	N2 In2 Br4	97.75(11)
O1 C6	1.406(6)	O4 In2 Br4	173.63(9)
		Br3 In2 Br4	94.58(2)
O3 Br4 (H-bond)	3.210(1)	O2 In1 O1	72.87(12)
O4 Br2 (H-bond)	3.279(1)	O2 In1 N1	144.40(14)
		O1 In1 N1	73.33(13)
		O2 In1 O3	81.37(13)
		O1 In1 O3	84.07(13)
		N1 In1 O3	84.36(15)
		O2 In1 Br1	113.28(9)
		O1 In1 Br1	167.48(9)
		N1 In1 Br1	98.00(11)
		O3 In1 Br1	86.12(10)
		O2 In1 Br2	91.41(9)
		O1 In1 Br2	92.34(9)
		N1 In1 Br2	100.83(11)
		O3 In1 Br2	172.61(10)
		Br1 In1 Br2	98.26(2)
		In1 O2 In2	107.29(13)
		C6 O1 In2	130.1(3)
		C6 O1 In1	121.2(3)
		In2 O1 In1	106.45(13)

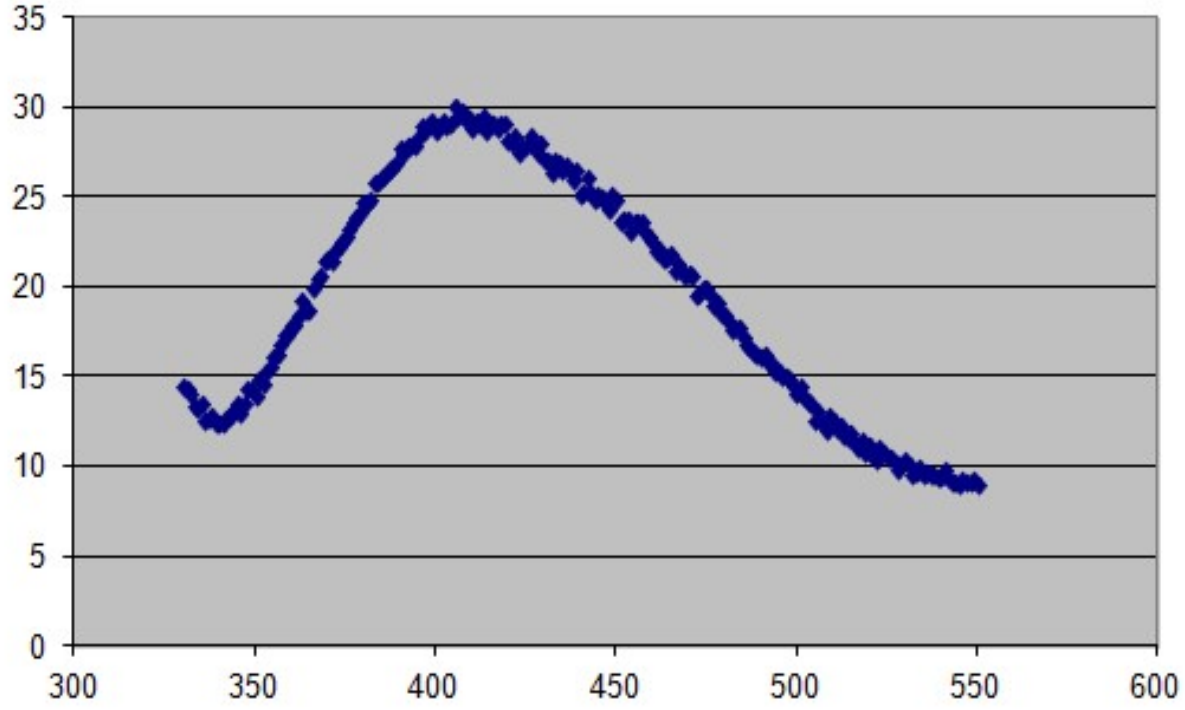

Fig. S1 Emission spectrum of solid $[In_2Br_4\{(py)(ph)CH(O)_2\}_2(EtOH)_2]$ (**4**) at room temperature under maximun excitation at 300 nm; the broad emission band is located at ~410 nm. This spectrum is in line with the fact that no satisfactory Raman spectrum of **4** could be recorded due to fluorescence. Despite the shorter excitation wavelength (300 nm) in this experiment, compared to the larger excitation laser wavelengths in the Raman experiments (514.5 nm and 632.8 nm), it is clear that a portion of fluorescence remains at λ>500 nm and thus fluorescence dominates the Raman effect.

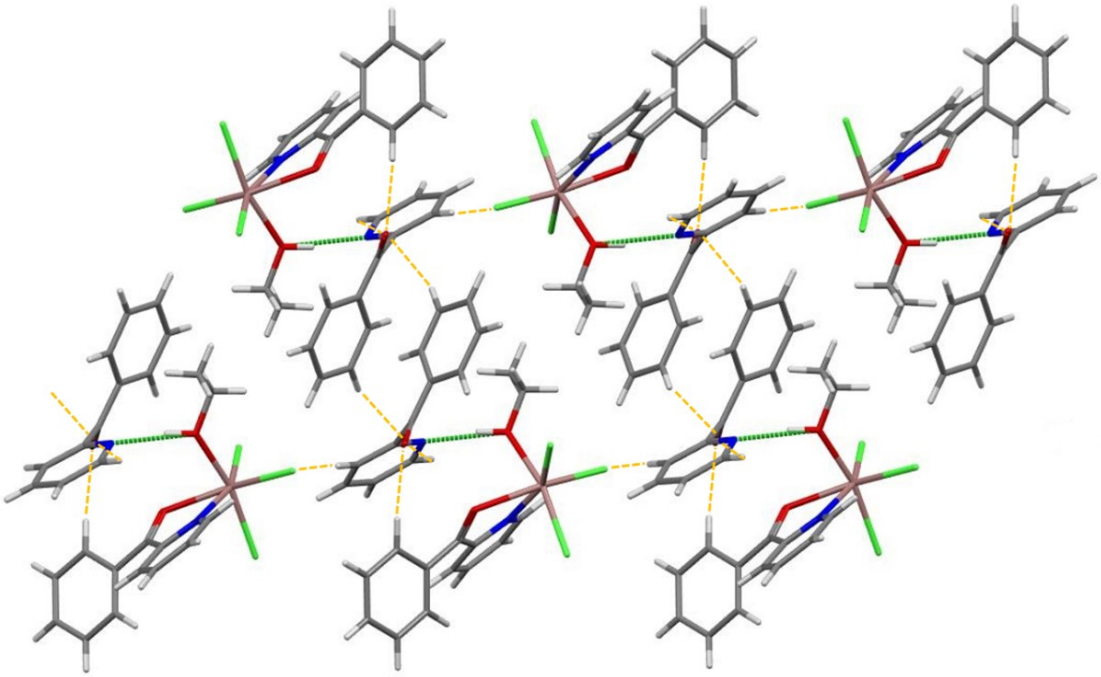

Fig. S2 Stick representation of the crystal structure of **1** along the (*ac*) plane, showing the packing of the complex molecules and the lattice (ph)(ph)CO molecules interacting through O-H···N H bonds (dashed green lines). The weak intermolecular C-H···O and C-H···Cl interactions are depicted in dashed orange lines. Colour code: C, grey; H, white; N, blue; O, red; Cl, light green; In, brown.

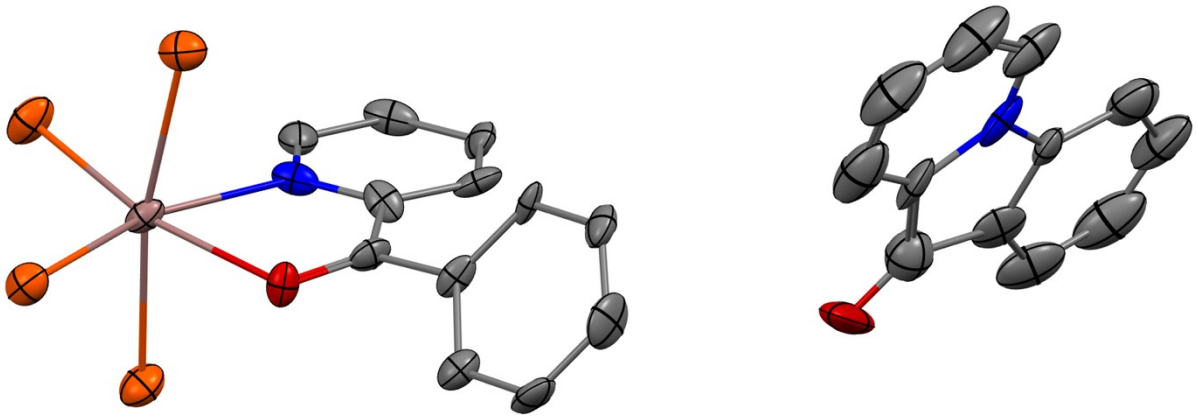

Fig. S3 Unlabelled ORTEP-type views of the octahedral complex anion $[InBr_4\{(ph)(ph)CO\}]^-$ and the cation L^+ that are present in the crystal structure of **3** at 120 K. Thermal ellipsoids are depicted at 50% probability level. H atoms are omitted for clarity. Colour code: C, grey; N, blue; O, red; Br, orange; In, brown.

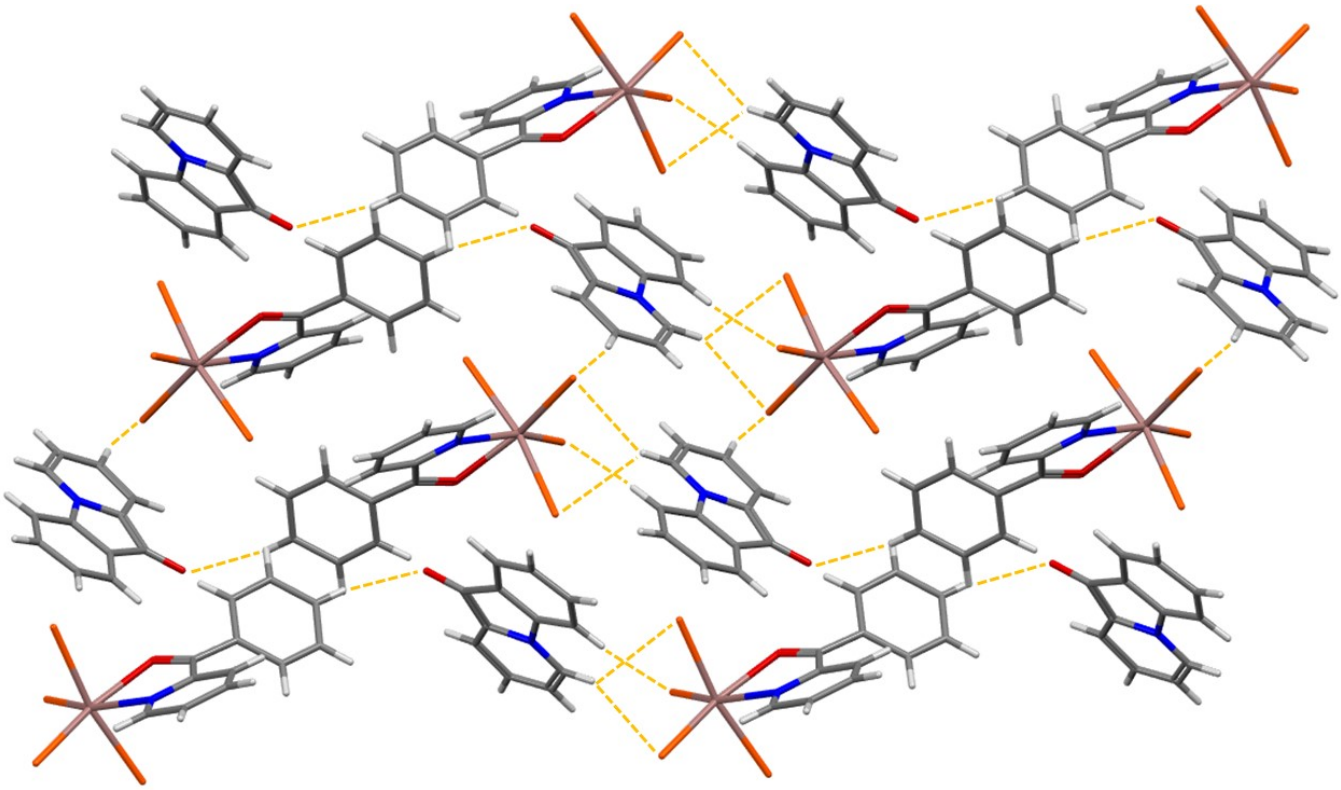

Fig. S4 Stick representation of the crystal structure of **3** along the (*ac*) plane, showing the packing of the complex anions and the organic cations. The weak intermolecular (a better description is "interionic") C-H···O and C-H···Br interactions are depicted in dashed orange lines. Colour code: C, grey; H, white; N, blue; O, red; Br, orange; In, brown.

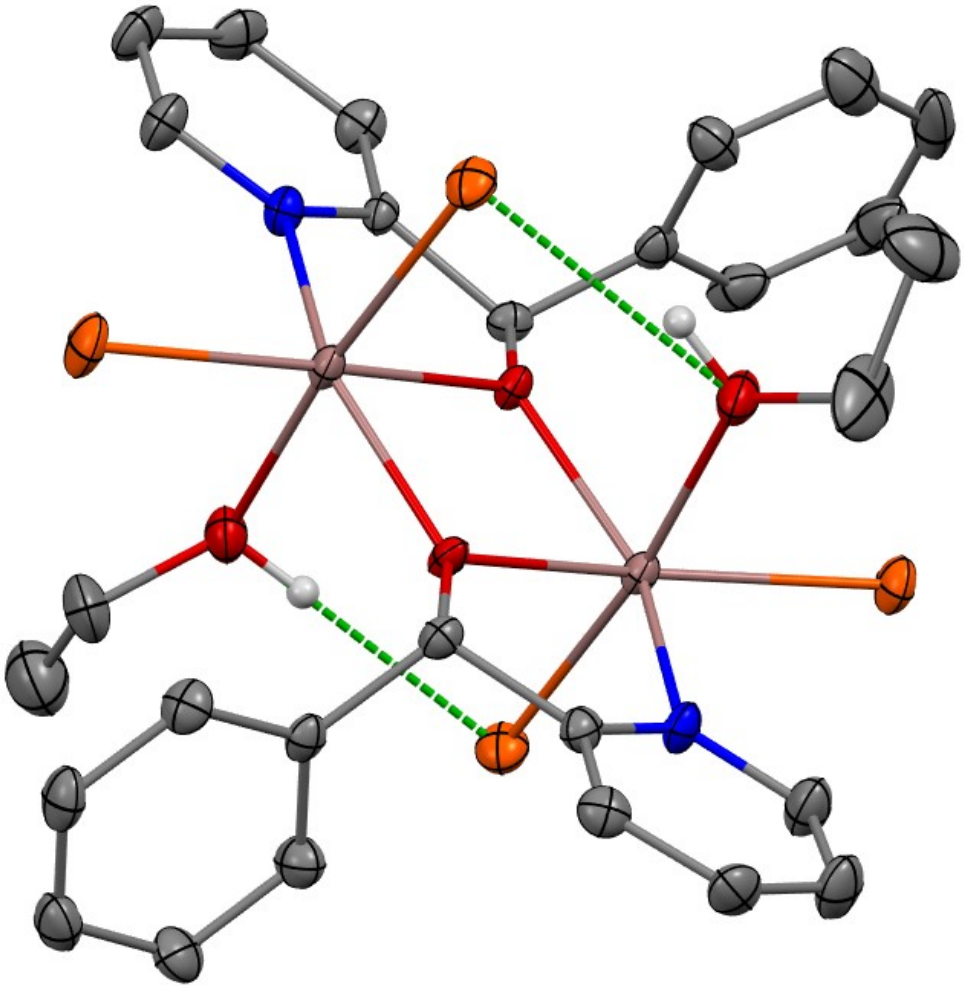

Fig. S5 Unlabelled ORTEP-type view of the dinuclear molecule that is present in the crystal structure of **4** at 120 K. Thermal ellipsoids are depicted at 50% probability level. The H bonds are represented by dashed green lines. H atoms are omitted for clarity, except those involved in the intramolecular $O_{ethanol}$-H···Br H bonds. Colour code: C, grey; N, blue; O, red; Br, orange; In, brown.

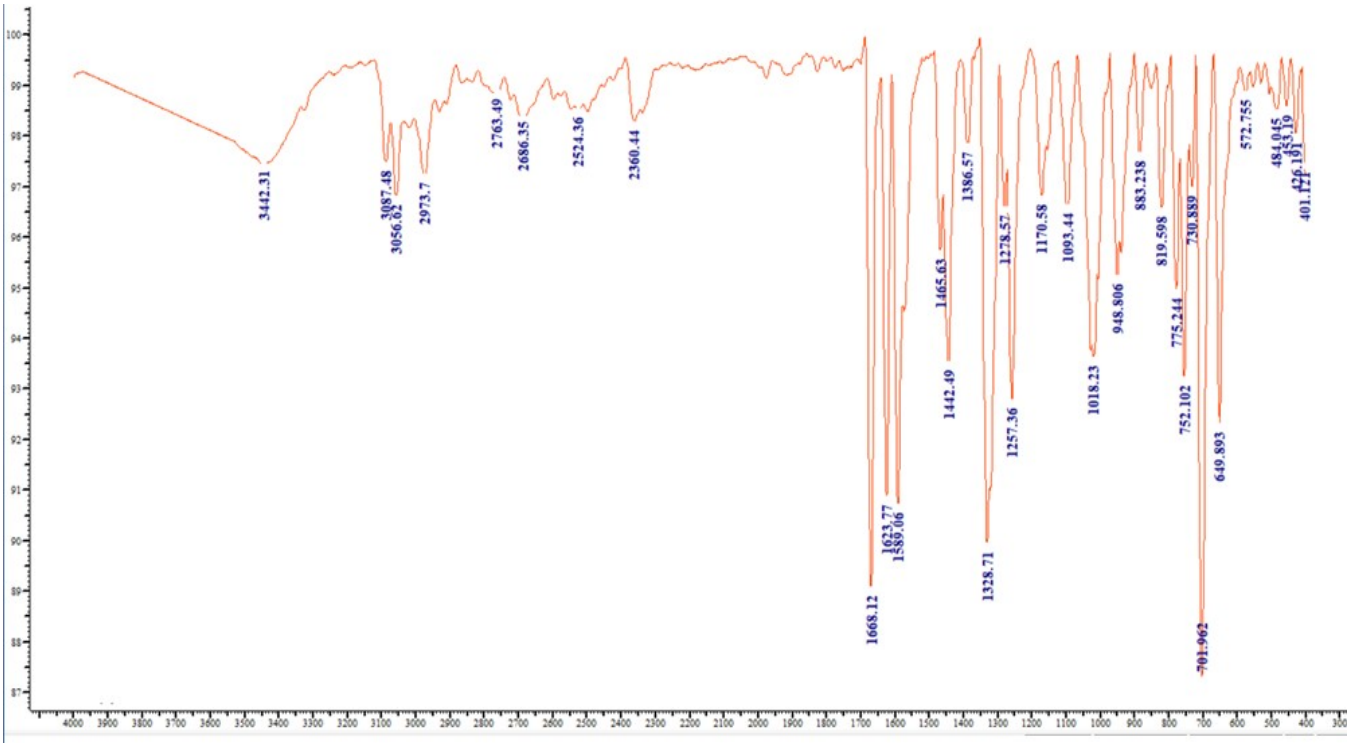

Fig. S6 The IR spectrum (KBr, cm^{-1}) of complex $[InCl_3\{(py)(ph)CO\}(EtOH)]\cdot\{(py)(ph)CO\}$ (**1**).

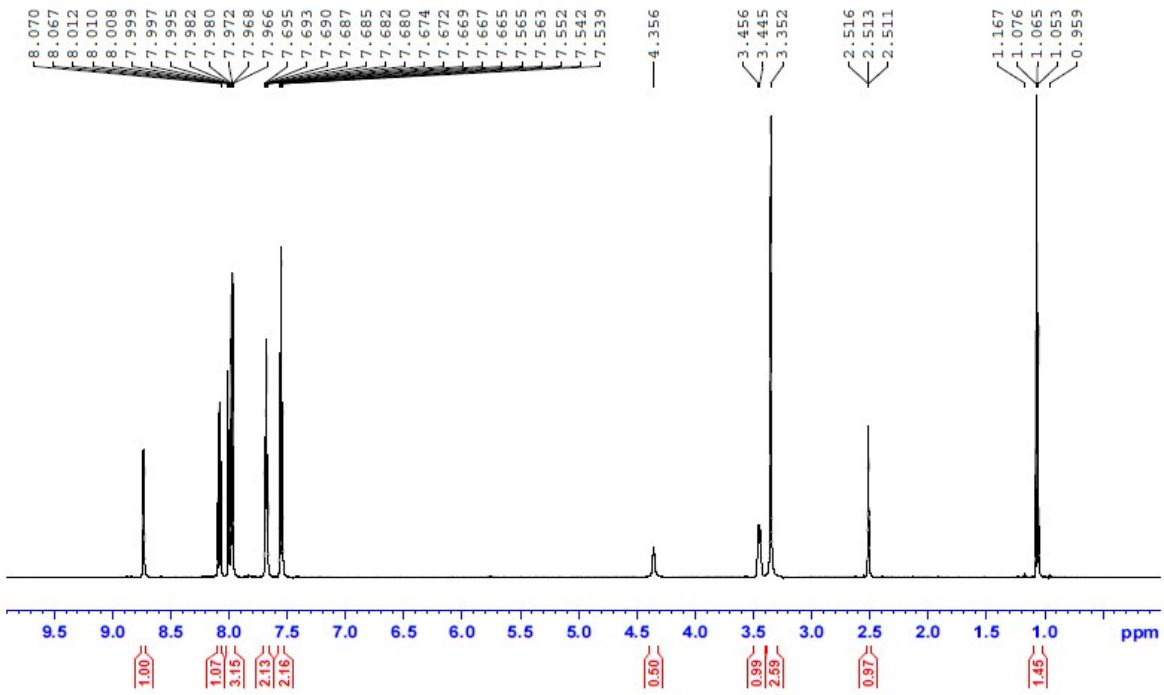

Fig. S7 The ^1H NMR spectrum (δ/ppm) of complex $[InCl_3\{(py)(ph)CO\}(EtOH)]\cdot\{(py)(ph)CO\}$ (**1**) in d_6-DMSO.

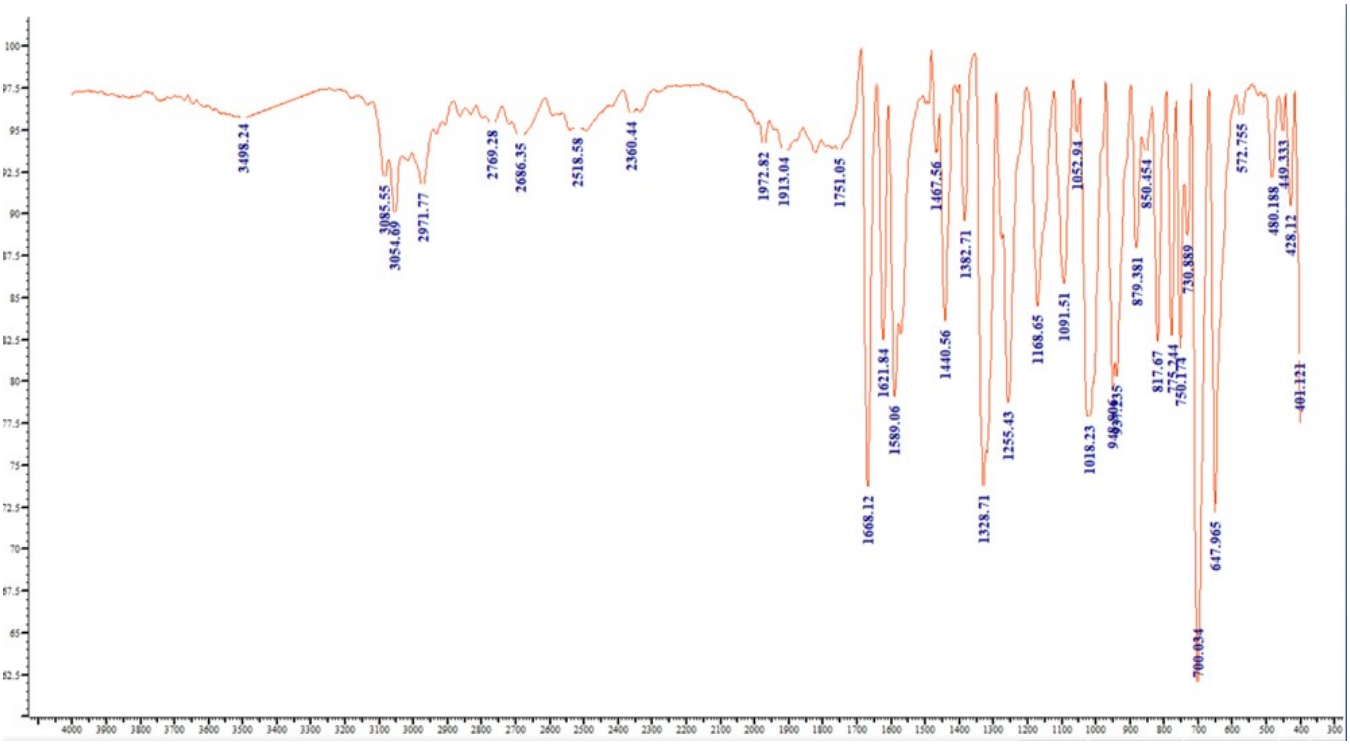

Fig. S8 The IR spectrum (KBr, cm^{-1}) of complex (L) $[InBr_4\{(py)(ph)CO\}]$ (**3**).

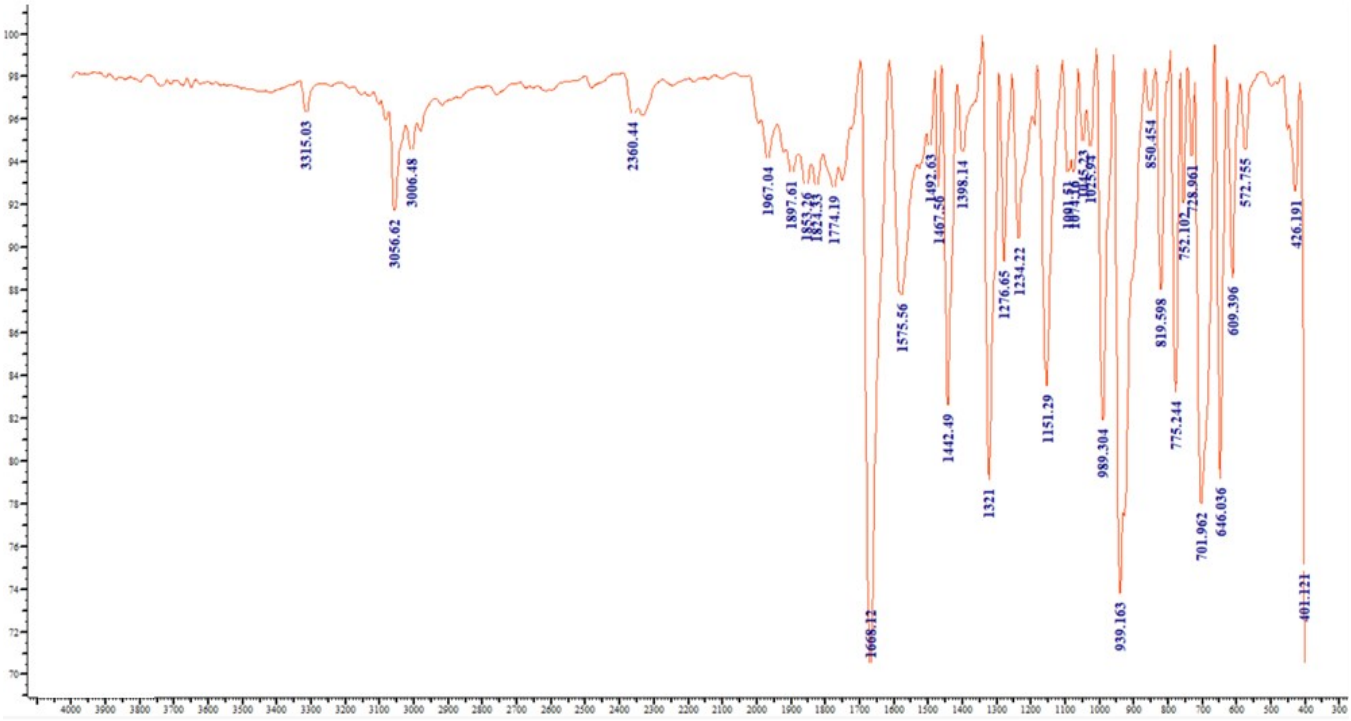

Fig. S9 The IR spectrum (KBr, cm^{-1}) of 2-benzoylpyridine, (py)(ph)CO.

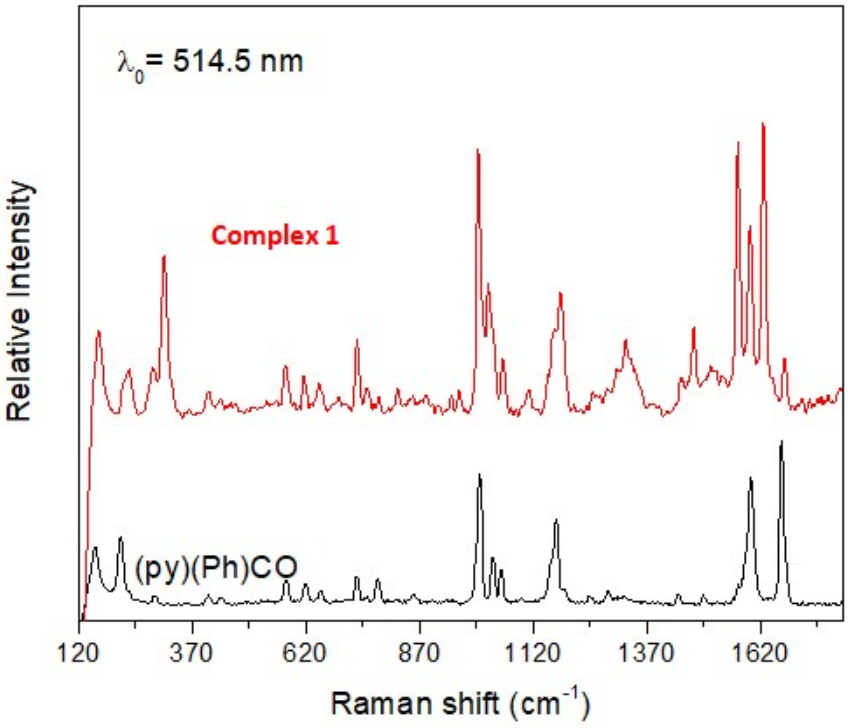

Fig. S10 The Raman spectra (cm^{-1}) of free (py)(ph)CO (bottom) and complex $[InCl_3\{(py)(ph)CO\}(EtOH)]\cdot\{(py)(ph)CO\}$ (**1**) in the region 1750-120 cm^{-1}.

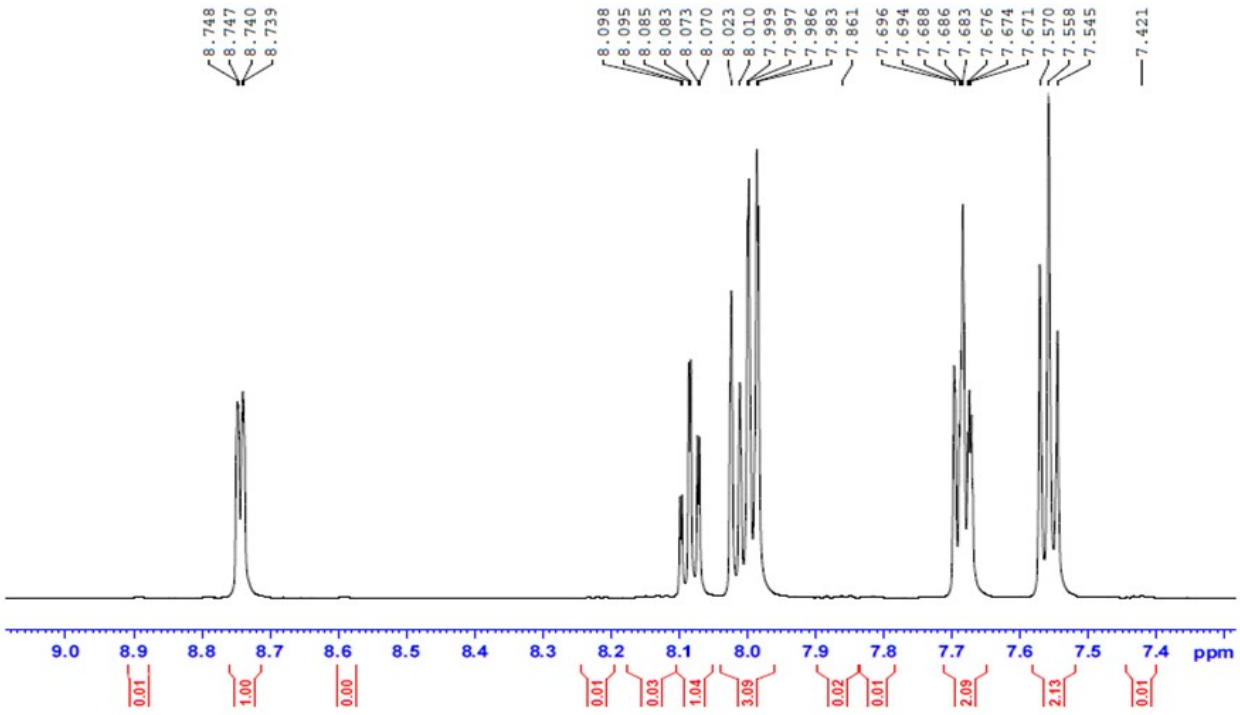

Fig. S11 The ^1H NMR spectrum (δ/ppm) of (py)(ph)CO in the aromatic region; the solvent used is d_6-DMSO.

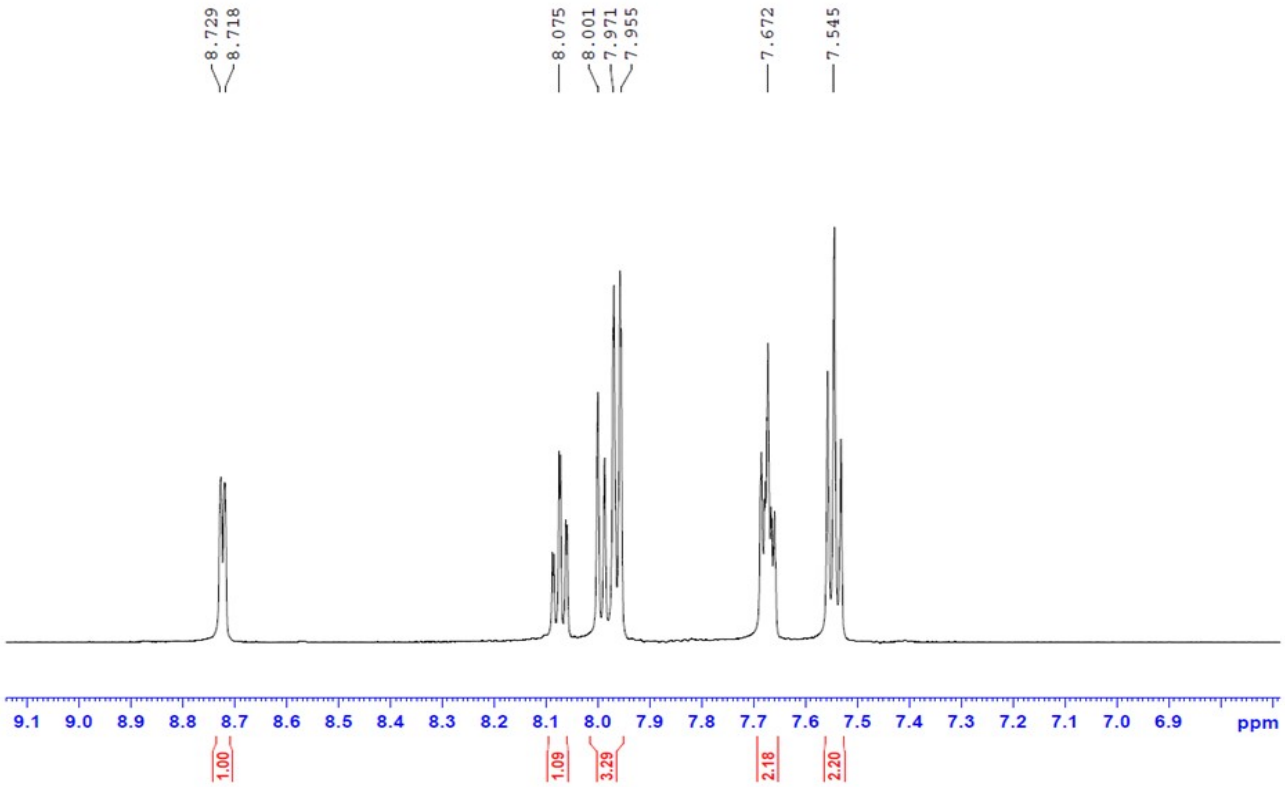

Fig. S12 The ^{1}H NMR spectrum (δ/ppm) of complex $[In_2Br_4\{(py)(ph)CH(O)_2\}_2(EtOH)_2]$ (**4**) in the aromatic region; the solvent used is d_6-DMSO.

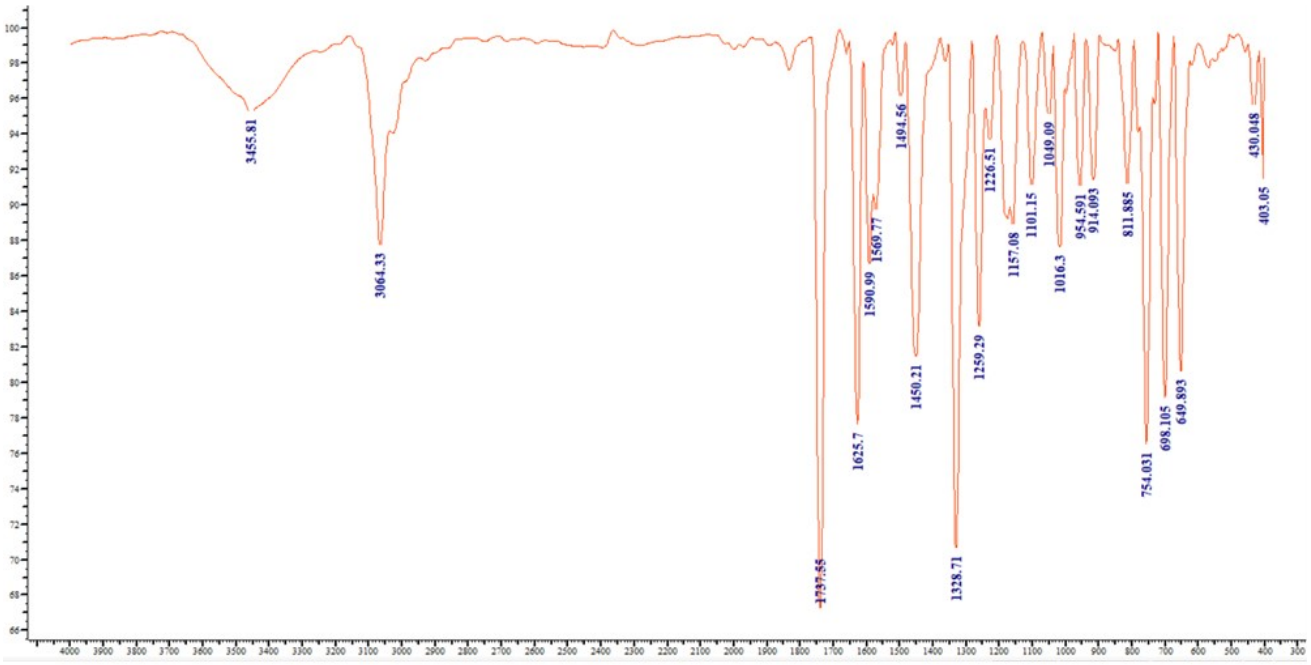

Fig. S13 The IR spectrum (KBr, cm^{-1}) of compound {(pyH)(ph)CO}Cl (**2**). The broad band at ~3440 cm^{-1} is due to residual EtOH from incomplete dryness of this particular sample (also evident in the ^{1}H and ^{13}C{^{1}H} NMR spectra.

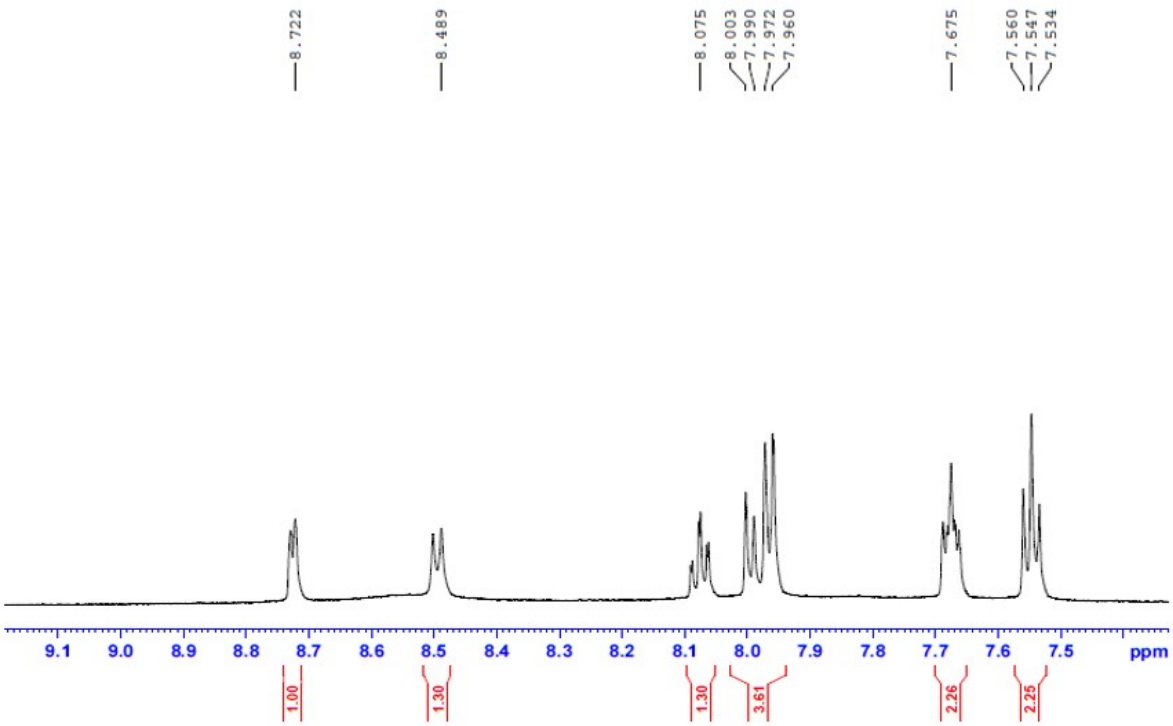

Fig. S14 The ^{1}H NMR spectrum (δ/ppm) of compound **2** in the 9.2-7.4 ppm region; the solvent used is d_6-DMSO.

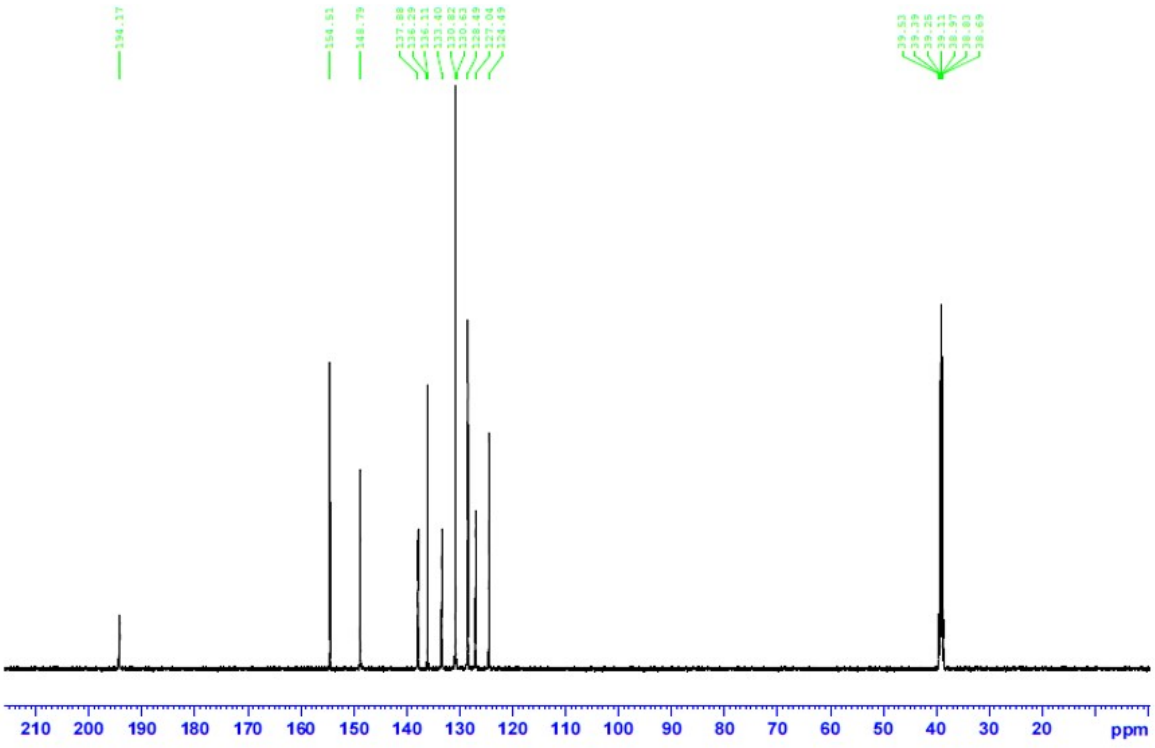

Fig. S15 The ^{13}C{^{1}H} NMR spectrum of (py)(ph)CO in d_6-DMSO; the signal at δ 39.2 ppm is due to the methyl carbons of the solvent.

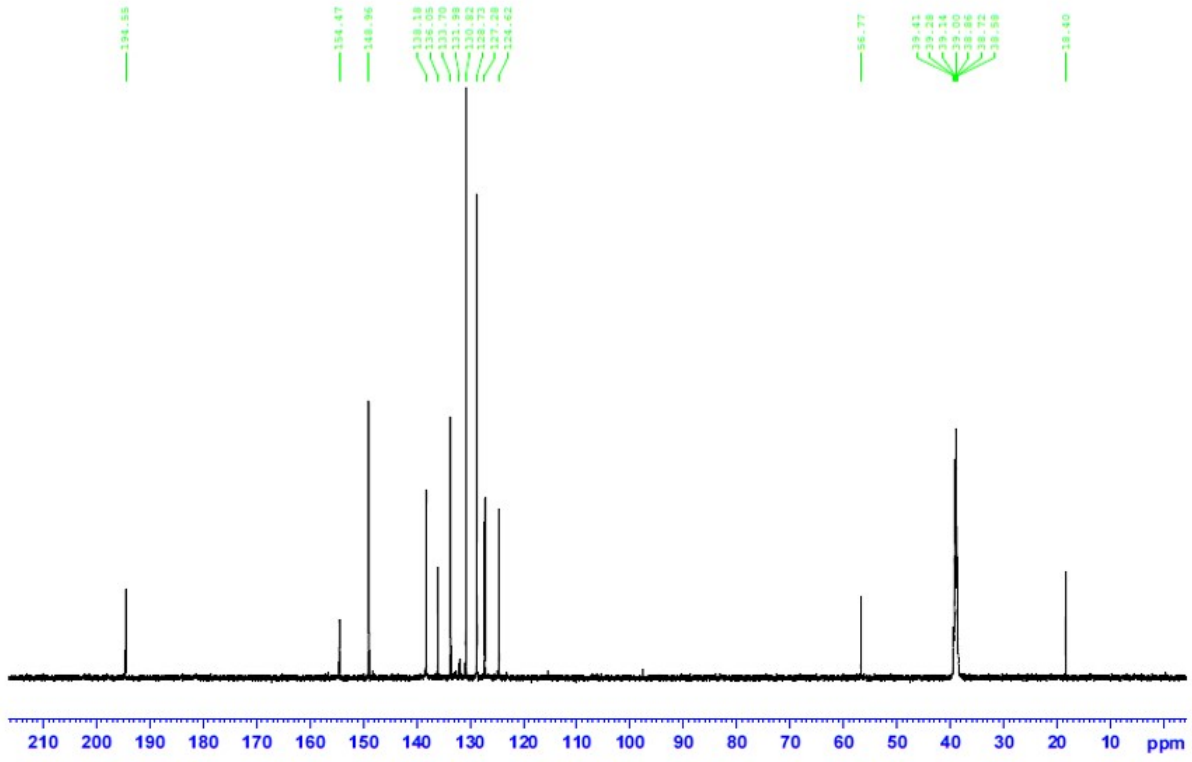

Fig. S16 The $^{13}C\{^{1}H\}$ NMR spectrum of (py)(ph)CO in d_6-DMSO; the signal at δ 39.1 ppm is due to the methyl carbons of d_6-DMSO. The signals at δ 56.8 and 18.4 ppm arise from the carbons of residual EtOH from incomplete dryness of this particular sample; the presence of EtOH in this sample is also evident in its ^{1}H NMR and IR spectrum (Fig. S13).

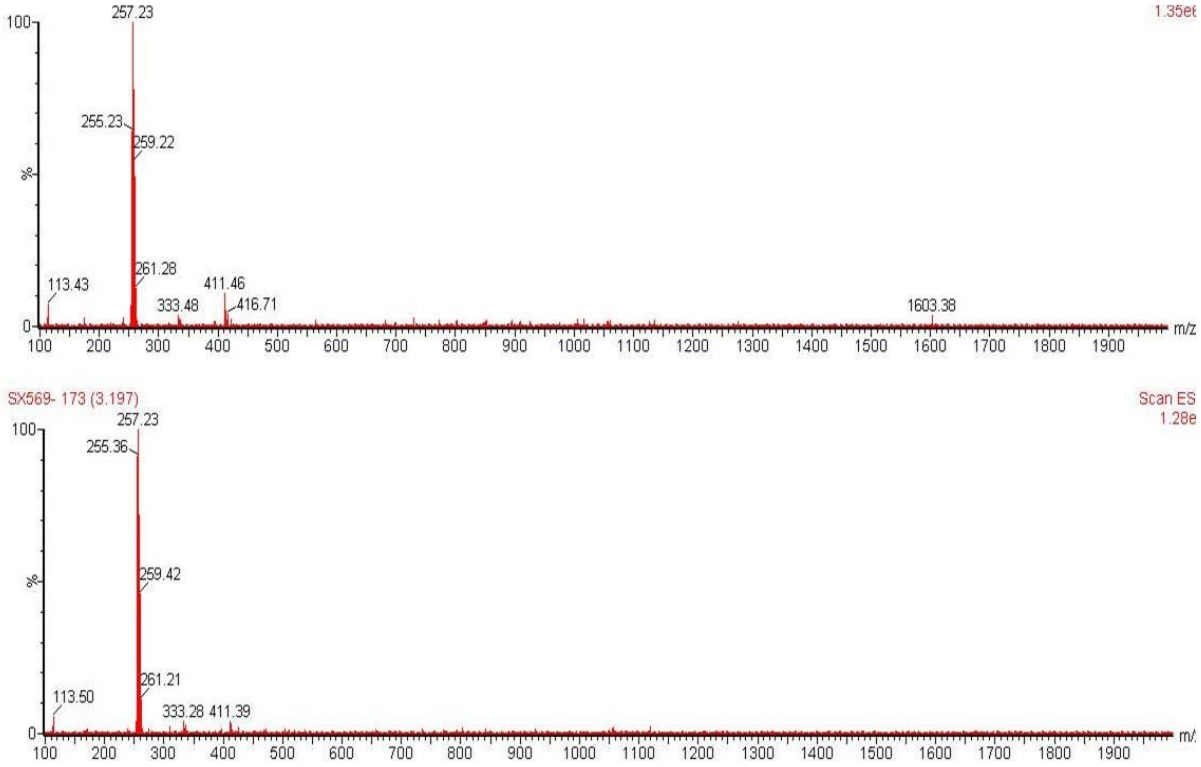

Fig. S17 The ESI-MS spectrum of {(pyH)(ph)CO}Cl (**2**) in the negative mode.